

ChemistrySelect

Extended π -Conjugated Pyrene Derivatives: Structural, Photophysical and Electrochemical Properties

--Manuscript Draft--

Manuscript Number:	slct.201600598R1
Article Type:	Full Paper
Corresponding Author:	Takehiko Yamato Saga University Saga, JAPAN
Corresponding Author E-Mail:	yamatot@cc.saga-u.ac.jp
Other Authors:	Xing Feng, PhD Nobuyuki Seto Chuan-Zeng Wang Taisuke Matsumoto, PhD Junji Tanaka, PhD Xian-Fu Wei, PhD Mark R. J. Elsegood, PhD Lynne Horsburgh, PhD Carl Redshaw, PhD
Keywords:	Pyrenes; Intramolecular charge-transfer; Single crystals; Luminescence material; Structure-property relationship
Manuscript Classifications:	Supramolecular Chemistry
Abstract:	This article presents a set of extended π -conjugated pyrene derivatives, namely 1,3-di(arylethynyl)-7-tert-butylpyrene, which were synthesized by a Pd-catalyzed Sonogashira coupling reaction of 1,3-dibromo-7-tert-butylpyrene with the corresponding arylethynyl group in good yields. Despite the presence of the tert-butyl group located at the 7-position of pyrene, X-ray crystallographic analyses show that the planarity of the Y-shaped molecules still exhibits strong face-to-face π - π stacking in the solid state; all of the compounds exhibit blue or green emission with high quantum yields (QYs) in dichloromethane. DFT calculations and electrochemistry revealed that this category of compound possesses hole-transporting characteristics. In addition, with strong electron-donating (-N(CH ₃) ₂) or electron-withdrawing (-CHO) groups in 2d or 2f, these molecules displayed efficient intramolecular charge-transfer (ICT) emissions with solvatochromic shifts from blue to yellow (green) on increasing the solvent polarity. Furthermore, the compounds 2d and 2f possess strong CT characteristics.
Response to Reviewers:	Dear editor Thank you very much for your E-mail about our manuscript, manuscript number: slct.201600598. We deeply appreciate for your acceptance. We have prepared all of the documents for the publication according to the comments from the editorial office. Thank you very much for your time and consideration. Yours sincerely, Prof. Dr. Takehiko Yamato (corresponding author) Department of Applied Chemistry Faculty of Science and Engineering Saga University Honjo-machi 1, Saga-shi, Saga 840-8502, Japan Fax: (internet.) + 81(0)952/28-8548 E-mail: yamatot@cc.saga-u.ac.jp

Section/Category:	Organic & Supramolecular Chemistry
Additional Information:	
Question	Response
Submitted solely to this journal?	Yes
Has there been a previous version?	No
Dedication	
Animal/tissue experiments?	No
If accepted, do you wish to publish your work in an open access format through OnlineOpen?	Yes
Was the work described in your manuscript funded by any of the following funding bodies? as follow-up to "If accepted, do you wish to publish your work in an open access format through OnlineOpen?"	No
Please select a Creative Commons license: as follow-up to "Was the work described in your manuscript funded by any of the following funding bodies?"	Creative Commons Attribution Non-Commercial NoDerivs License (CC-BY-NC-ND)

Extended π -Conjugated Pyrene Derivatives: Structural, Photophysical and Electrochemical Properties

Xing Feng,^{*[a,b]} Nobuyuki Seto,^[a] Chuan-Zeng Wang,^[a] Taisuke Matsumoto,^[c] Junji Tanaka,^[c] Xian-Fu Wei,^[b] Mark R. J. Elsegood,^[d] Lynne Horsburgh,^[d] Carl Redshaw^[e] and Takehiko Yamato^{*[a]}

Dedication ((optional))

Abstract: This article presents a set of extended π -conjugated pyrene derivatives, namely 1,3-di(arylethynyl)-7-*tert*-butylpyrene, which were synthesized by a Pd-catalyzed Sonogashira coupling reaction of 1,3-dibromo-7-*tert*-butylpyrene with the corresponding arylethynyl group in good yields. Despite the presence of the *tert*-butyl group located at the 7-position of pyrene, X-ray crystallographic analyses show that the planarity of the Y-shaped molecules still exhibits strong face-to-face π - π stacking in the solid state; all of the compounds exhibit blue or green emission with high quantum yields (QYs) in dichloromethane. DFT calculations and electrochemistry revealed that this category of compound possesses hole-transporting characteristics. In addition, with strong electron-donating (-N(CH₃)₂) or electron-withdrawing (-CHO) groups in **2d** or **2f**, these molecules displayed efficient intramolecular charge-transfer (ICT) emissions with solvatochromic shifts from blue to yellow (green) on increasing the solvent polarity. Furthermore, the compounds **2d** and **2f** possess strong CT characteristics.

Introduction

Large π -conjugated organic materials have attracted increasing attention in recent years, due to facile band-gap and colour control by structural modification, which makes them suitable for potential application in high performance organic electronics,¹ such as organic light emitting diodes (OLEDs),² liquid-crystal

displays,³ organic field effect transistors (OFETs)^{4,5} and organic photovoltaic cells (OPVs),⁶ as well as optical storage devices.⁷ Extension of the π -conjugation chromophores contributes to a lowering of the HOMO-LUMO gap, leading to a red-shift in absorption and emission spectra with increasing fluorescence quantum yields. In addition, molecules which possess π -conjugation with a planar structure would enhance charge carrier transport in optoelectronic applications by self-assembly *via* intermolecular π - π stacking.⁸

Pyrene⁹ is made up of four fused aromatic rings with a large π -electron system, which exhibits good solution-processable properties with an excellent blue emission spectrum (with a long excited-state lifetime, high fluorescence intensity and quantum yield). However, the development of pyrene as a host material in blue light-emitting diodes is scarce, due to its tendency to readily aggregate in most media. Several research groups including ours have reported many new types of pyrene derivatives, and various substituent groups have been attached to the pyrene core by -C-C-, -C-N- or -C \equiv C- bonds for suppressing excitation emission.¹⁰⁻¹⁵ Some ethynyl-substituted pyrene-based compounds displayed more intriguing fluorescence characteristics, for instance, Ziessel *et al* reported a greenish luminescent 1,3,6,8-tetra-(4-ethynylphenylaminoacyl)pyrene with stable liquid crystalline properties for the fabrication of OLED-like devices;¹⁶ Kim and coworkers synthesized a series of 1,3,6,8-tetrakis(ethynyl)pyrenes functionalized with varying numbers of *N,N*-dimethylaniline and 1-(trifluoromethyl)benzene moieties as peripheral electron-donors and acceptors for chemiluminescent (ECL) active materials, that exhibited enhanced charge transfer compared with 1,3,6,8-tetra-*N,N*-dimethylaniline (or 1,3,6,8-tetra-trifluoromethylbenzene).^{17,18} Interestingly, Adachi *et al* have designed a number of inverted singlet-triplet (iST) pyrene-based derivatives, and the electronic structures, spin-orbit couplings, transition dipole moments, and vibronic couplings have been investigated by theoretical calculations.¹⁹

Generally, an acetylene group is one option among other (such as ethylene) choice to extend the π -conjugation of molecular skeletons, and the advantage over ethylene linker is a better stability, in addition, it's very convenient to prepared this kind of compounds by Pd-catalyzed coupling reaction. Previously, in our laboratory, we synthesized cruciform-shaped and hand-shaped architectures incorporating π -conjugated alkynylpyrenes as highly efficient blue emissive materials by the Sonogashira cross-coupling reaction.^{20,21} The optical properties of both types of pyrene-based material exhibited pure blue fluorescence with good quantum yield, as well as similar crystal packing in the solid-state. Our recent report on the synthesis of 1,3-dibromo-7-*tert*-butylpyrene (**1**)²² prompted us to further explore 1,3-bis(arylphenyl)pyrenes as blue emissive materials.

[a] Dr. X. Feng, N. Seto, C.-Z. Wang, Prof. Dr. T. Yamato
Department of Applied Chemistry, Faculty of Science and Engineering
Saga University

Honjo-machi 1, Saga 840-8502 Japan
E-mail: hyxhn@sina.com, yamatot@cc.saga-u.ac.jp

[b] Dr. X. Feng, Prof. X.-F. Wei
School of Printing and Packaging Engineering
Beijing Institute of Graphic Communication
1 Xinghua Avenue (Band Two), Daxing, Beijing, 102600, P. R. China
E-mail: hyxhn@sina.com

[c] Dr. J. Tanaka, Dr. T. Matsumoto
Institute of Materials Chemistry and Engineering
Kyushu University
6-1, Kasugakoen, Kasuga 816-8580, Japan

[d] Dr. M. R. J. Elsegood, Dr. L. Horsburgh
Chemistry Department
Loughborough University
Loughborough, LE11 3TU, UK

[e] Prof. Dr. C. Redshaw
Department of Chemistry
The University of Hull
Cottingham Road, Hull, Yorkshire HU6 7RX, UK

Supporting information for this article is given via a link at the end of the document. ((Please delete this text if not appropriate))

This is the peer reviewed version of the following article: X. Feng, N. Seto, C.-Z. Wang, T. Matsumoto, J. Tanaka, X.-F. Wei, M. R. J. Elsegood, L. Horsburgh, C. Redshaw, T. Yamato, *ChemistrySelect* 2016, 1, 1926, which has been published in final form at <http://dx.doi.org/10.1002/slct.201600598>. This article may be used for non-commercial purposes in accordance With Wiley Terms and Conditions for self-archiving.

The arylphenyl groups located at the 1,3-positions were twisted by a considerable angle relative to the pyrene core, a feature that can play a curial role in hindering intermolecular interactions in the solid-state. In this article, a series of Y-shaped, extended π -conjugated pyrene derivatives have been synthesized by a Pd-catalyzed Sonogashira cross-coupling reaction using 1,3-dibromo-7-*tert*-butylpyrene and corresponding arylethynyl groups in reasonable yield. We anticipated that the extended π -conjugated pyrene derivatives would exhibit interesting topological structures, leading to attractive photophysical properties, as well being air-stable. Indeed, the designed π -conjugated molecules showed interesting CT characteristics in polar solvents as expected. Furthermore, we investigated the effect of the various substituents and substitution positions of the (arylethynyl)pyrenes for optical properties and crystal packing.

Results and Discussion

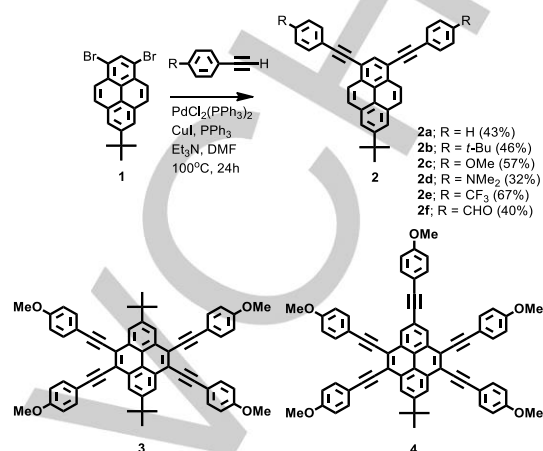
Synthesis and characterization

The synthesis of the Y-shaped arylethynyl-substituted pyrenes **2** are shown in Scheme 1. The target arylethynyl pyrenes **2** were obtained in 32–67% yield through a Sonogashira coupling reaction between **1** and the corresponding arylethylenes. All of the new pyrene derivatives **2** have been characterized by $^1\text{H}/^{13}\text{C}$ NMR spectroscopy (Figure S1), HR-MS and elemental analysis. Y-shaped compounds **2** with arylethynyl groups display good air-stability and solubility properties in common solvents, such as dichloromethane (CH_2Cl_2), *N,N*-dimethylformamide (DMF), tetrahydrofuran (THF) and methanol (CH_3OH). Moreover, the structures of **2c** (two polymorphs), **2d** and **2f** were further confirmed by X-ray single crystal diffraction. Very recently, compounds **2a** and **2b** have been prepared by cooper et al as key intermediation^[23] Herein, the effect of the substituents on the crystal packing, photophysical properties and electrochemistry has been further investigated in detail; for comparison, two position-dependent arylethynyl-functionalized pyrenes **3** and **4** are illustrated in Scheme 1. This work allows us to fully understand the effect of the various substituents and the relationship between molecular structure and optical properties.

Single crystal X-ray crystallography

Single crystals of the extended π -conjugated Y-shaped pyrene derivatives **2c** were obtained from $\text{MeOH}/\text{CHCl}_3$ or hexane/ CH_2Cl_2 , **2d-CHCl}_3** from CHCl_3 and **2f** from CH_2Cl_2 /benzene by slow evaporation at room temperature. All of the compounds crystallize in the *triclinic* crystal system with space group $P\bar{1}$. Compound **2c** was obtained as two different polymorphs. Number of reports showed that pyrene derivatives with terminal of methoxyphenyl moieties trends to more easily to form good quality single crystal for X-ray crystallography. So this experience allows us to design pyrenes for insight into investigating the relationship between position-dependent, molecular conformation and the optical properties by using X-ray

diffraction equipment. The molecular structures are shown in Figure 1 and Figure S2 and the crystallographic data is listed in Table 1.



Scheme 1. The synthetic route to π -conjugated pyrene derivatives **2**, and the cruciform-shaped and hand-shaped pyrenes **3** and **4** for comparison.

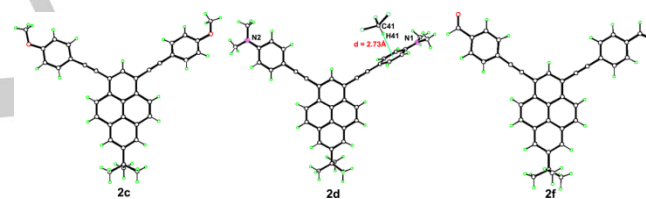


Figure 1. The molecular structures of **2c**, **2d-CHCl}_3** and **2f**.

As shown in Figure 2, the structure of **2c** displays face-to-face π -stacking at a distance of 3.54 Å, which involves 14 carbons in each pyrene molecule.²⁴ One ethynylphenyl substituent is coplanar with the pyrene core, whilst another forms a twist angle of 28.4°. A number of $\pi\cdots\pi$ stacking interactions between the phenyl rings and the neighbouring pyrene core were observed (3.32 Å). In addition, another weak but important interaction involves the methoxyl group, which has a contact with the next layer of the ethynyl fragment of pyrene via a C–H $\cdots\pi$ interaction (2.42 Å).

Similarly, the polymorphs of **2c** were crystallized from hexane/ CH_2Cl_2 solution. The X-ray structure determinations revealed that the **2c** belongs to the same space group as **2c**. The crystal packing analysis shows that polymorphs **2c** were arranged similar as **2c**. There is a fine distinction between both crystals are that the asymmetric unit cell of **2c** contained two molecules, whereas the crystals of **2c** were found to contain one molecule in the asymmetric unit. (See supporting information)

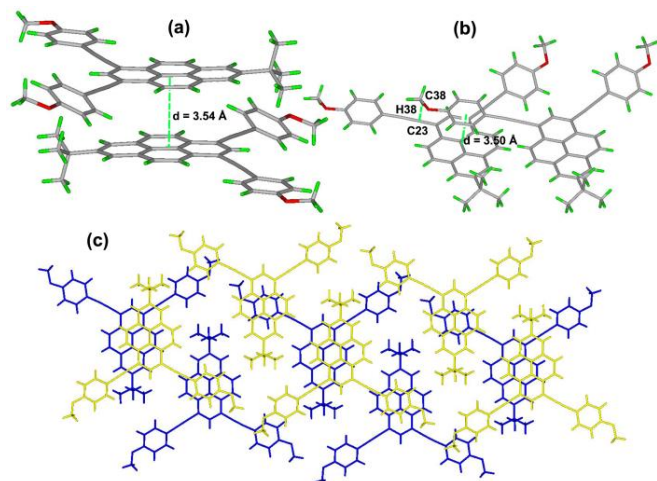


Figure 2. X-ray crystal structure representations of **2cl**, illustrating (a) and (b) the co-facial π -stacking structures and (c) the principal intermolecular packing interactions.

Table 1. Summary of crystal data for the π -conjugated molecules **2cl**, **2cII**, **2d**· CHCl_3 and **2f**.

Complex	2cl	2cII	2d	2f
Empirical formula	$\text{C}_{38}\text{H}_{30}\text{O}_2$	$\text{C}_{38}\text{H}_{30}\text{O}_2$	$\text{C}_{40}\text{H}_{36}\text{N}_2 \cdot \text{CHCl}_3$	$\text{C}_{38}\text{H}_{26}\text{O}_2$
Formula weight	518.62	518.62	664.07	514.59
Crystal system	Triclinic	Triclinic	Triclinic	Triclinic
Space group	$P \bar{1}$	$P \bar{1}$	$P \bar{1}$	$P \bar{1}$
a [Å]	8.926(2)	8.902(2)	10.8101(12)	8.9354(5)
b [Å]	12.408(3)	12.088(3)	11.1244(12)	11.8785(9)
c [Å]	13.559(3)	27.070(8)	14.3383(16)	13.0754(6)
α [°]	99.758(9)	101.774(18)	91.4712(18)	97.029(5)
β [°]	100.102(9)	93.904(19)	91.6750(18)	102.787(4)
γ [°]	98.809(8)	100.502(18)	101.8031(17)	100.349(5)
Volume[Å ³]	1430.9(6)	2787.1(13)	1686.2(3)	1312.22(14)
Z	2	4	2	2
λ	0.71073	1.54184	0.71073	1.54184
Dcalcd[Mg/m ³]	1.204	1.236	1.308	1.302
temperature [K]	293(2)	296(2)	150(2)	100(2)
measured reflns	12587	36576	19720	7853
unique reflns	4927	9802	9976	5075
obsd reflns	2470	4722	7491	3892
Parameters	362	731	552	462
R (int)	0.0337	0.0548	0.0184	0.0219
R [$> 2\sigma(I)$] ^a	0.0774	0.0887	0.0457	0.0545
$wR2$ [all data] ^b	0.2342	0.2725	0.1344	0.1687
GOF on F^2	1.007	1.010	1.059	1.052

^a Conventional R on $F_{\text{hk}}|$: $\sum ||F_o| - |F_c|| / \sum |F_o|$. ^b Weighted R on $|F_{\text{hk}}|^2$: $\sum [w(F_o^2 - F_c^2)]^2 / \sum [w(F_o^2)]^{1/2}$

Figure 3 reveals that the asymmetric unit contains a molecule of **2d** and a chloroform linked by a $\text{C-H} \cdots \pi$ interaction at a distance of 2.41(2) Å. Unlike the situation above for **2cl**, where the *p*-methoxyphenylethynyl moieties and the pyrene ring are almost coplanar, here for **2d**, the torsional angle between the pyrene unit and one of the the 4-(*N,N*-dimethylamino)-phenylethynyl fragments is close to perpendicular with a twist angle of 87.87(3)°. Moreover, two neighbouring pyrene moieties are presented with displaced face-to-face patterns forming a star-shaped architecture in the solid-state; the $\pi \cdots \pi$ stacking interactions are approximately 3.37 Å (Figure 3a). In addition, the terminal phenyl groups of neighbouring molecules were connected by $\pi \cdots \pi$ stacking interactions with a distance of 2.89 Å (Figure 3b).

From the packing pattern, a two-dimensional supramolecular network was constructed by these complicated $\pi \cdots \pi$ stacking interactions, and the CHCl_3 molecules were captured in the molecular voids²⁵ by $\text{C-H} \cdots \pi$ interactions.

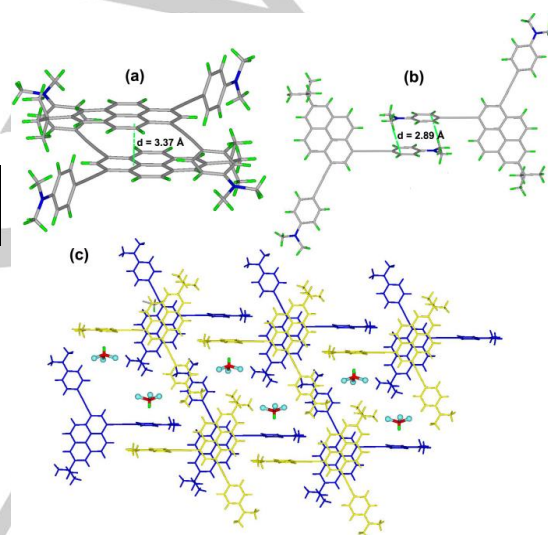


Figure 3. X-ray crystal structure representations of **2d**· CHCl_3 , illustrating (a) and (b) the co-facial π -stacking structures and (c) CHCl_3 molecules were captured in voids supported by $\text{C-H} \cdots \pi$ interactions.

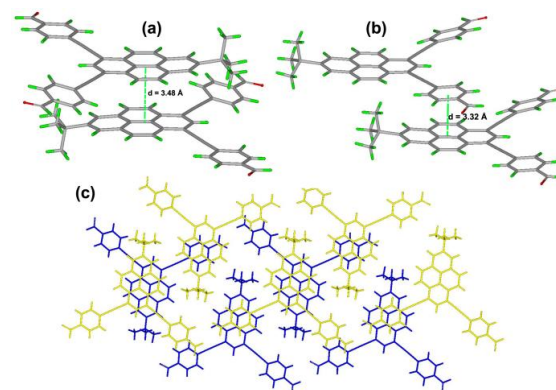


Figure 4. X-ray crystal structure representations of **2f**, illustrating (a) and (b) the detail of the cofacial π -stacking structures and (c) the principal intermolecular packing interactions.

The asymmetric unit of **2f** contains one molecular with no solvent of crystallisation. As shown in Figure 4, **2f** displays a slightly curved core structure (torsional angle $<5^\circ$) with shallow twist angles of 17.57(9) and 3.03(8)° between the pyrene core and the terminal phenyl groups. Obviously, the planar molecular structure would tend to form strong co-facial $\pi\cdots\pi$ stacking, and

the pairs of pyrene units arrange in head-to-tail stacking via a centre of symmetry by $\pi\cdots\pi$ interactions (3.48 Å). In addition, the pyrene units and the adjacent phenyl rings display face-to-face $\pi\cdots\pi$ stacking at a distance of 3.32 Å. Interestingly, from the packing structure of **2f**, there are two key $\pi\cdots\pi$ interactions leading to a three dimensional infinite supramolecular array.

Table 2. The photophysical and electrochemical properties of compounds **2**.

R	$\lambda_{\text{max abs}}^{\text{a}}$ nm	$\lambda_{\text{max PL}}^{\text{a}}$ (nm)	Log ϵ	$\phi_{\text{f}}^{\text{a}}$	LUMO (eV)	HOMO (eV)	Energy gap (eV)	τ_{ns}	T_{m}^{f}	T_{d}^{g}
2a	406	421 (325)	4.87	0.93	-2.01 ^b (-2.41) ^c	-5.01 ^b (-5.34) ^d	2.99 ^b (2.93) ^e	2.89a	198	479
2b	409	423 (330)	4.88	0.93	-1.93 (-2.39)	-4.93 (-5.31)	2.99 (2.92)	2.93	288	469
2c	412	427 (333)	4.82	0.94	-1.85 (-2.37)	-4.79 (-5.27)	2.94 (2.90)	2.94	195	449
2d	431	517 (380)	4.74	0.86	-1.63 (-2.61)	-4.46 (-5.27)	2.83 (2.67)	3.51	237	440
2e	411	427 (313)	4.80	0.91	-2.37 (-2.42)	-5.33 (-5.32)	2.97 (2.90)	2.48	220	469
2f	425	485 (363)	4.77	0.80	-2.56 (-)	-5.39 (-)	2.83 (2.77)	nd	nd	nd

^a Measured in dichloromethane at room temperature. ^b DFT/B3LYP/6-31G* using Gaussian. ^c Calculated from the empirical formulae HOMO = $-(E_{\text{ox}}+4.8)$, ^d LUMO = HOMO + E_{g} , ^e Calculated from λ_{edge} , ^f Melting temperature (T_{m}) obtained from differential scanning calorimetry (DSC) measurement. ^g Decomposition temperature (T_{d}) obtained from thermogravimetric analysis (TGA), nd: not measured.

Furthermore, in the packing structure of **3**, the four phenyl rings are not coplanar with the central pyrene; the two unique dihedral angles are 18.3 and 23.6°. As shown in Figure 5, two neighbouring pyrene moieties possess a centroid-to-centroid distance of 5.99 Å. No significant π -stacking interactions between the pyrene rings were observed and molecules adopt a herringbone packing motif. Non-covalent interactions play an important role in the stacking of the structures.

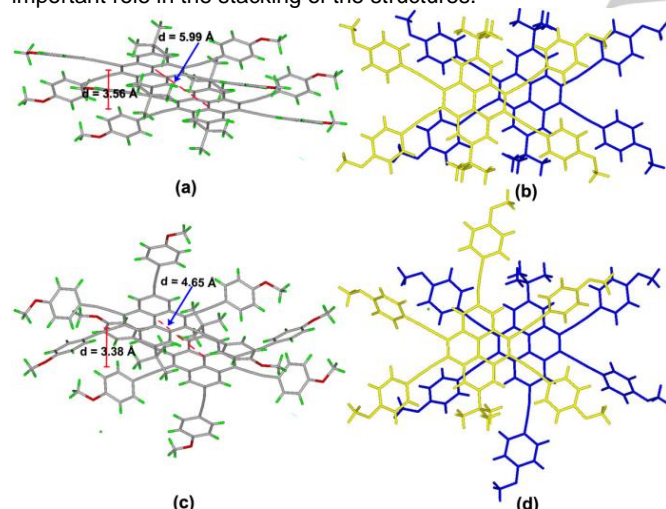


Figure 5. The packing structure (a) side view and (b) top view for **3** and (c) side view and (d) top view for **4**.

However, in compound **4**, when a *p*-methoxyphenyl moiety is located at the 7-position of pyrene, it is almost coplanar with the pyrene ring. The other four phenyl rings at the 4,5,9,10-positions of the pyrene form dihedral angles of between 6.1 and 47.3°, and two neighbouring pyrene moieties adopt a slipped face-to-face motif with off-set head-to-tail stacking with a centroid-to-centroid distance of 4.65 Å. Each molecule of **4** displays 24-point π - π stacking with molecules above and below using both

the pyrenyl and ethynyl carbon with intermolecular distances of 3.42–3.58 Å.

As mentioned above, the crystal packing is clearly marked off between pyrenes **2**, **3** and **4**. With the substituted group number increasing, the crystal packing has been transformed from face-to-face $\pi\cdots\pi$ stacking with off-set head-to-tail stacking to a herringbone arrangement on going from **2**, **3** to **4**. On the other hand, bulkier *tert*-butyl groups located at the 7-position of pyrene can play a more crucial role in hindering the $\pi\cdots\pi$ stacking versus the arylethynyl-substituted group. In compound **4**, due to the nodal planes passing through the 7-position of the pyrene, the phenyl moiety attached at this position would be of limited impact for the crystal arrangement, as well as the electronic interactions.²⁶ The planar molecular structure of the pyrene derivatives **2**, **3** and **4** is beneficial for extending π -conjugation and improving the optical density, which can lead to special photophysical properties both in solution and in the solid state.

Photophysical properties

The absorption spectra of the title compounds **2** in dilute dichloromethane are presented in Figure 6 and the optical data is summarized in Table 2. The maximum absorption wavelength of the ethynylpyrenes **2** is exhibited at least ca. 68 nm red-shifted compared with 2-*tert*-butylpyrene (338 nm).¹⁵ Notably, the photophysical properties are highly dependent on the substituent units present. Y-shaped **2a–c** and **2e** show similar absorption behaviour and exhibit two prominent absorption bands in the regions 300–350 nm and 375–425 nm, respectively. For **2d** and **2f**, the maximum absorption wavelength has obviously red-shifted (~19 nm) relative to **2a**, arising from the intramolecular charge transfer (ICT) increase. Indeed, both **2d** and **2f** feature a broader and intense absorption in the long wavelength region 475–525 nm, indicating that the molecules tend to be more coplanar between the pyrene core and terminal ethynylphenyl groups by extending the π -conjugation, which is consistent with the crystallographic results. With an increased

length of π -conjugation, the molar absorption coefficients (ϵ) of **2d** and **2f** are lower than the others observed.

Especially, the 1,3-bis(4-methoxyphenylethynyl)pyrene **2c** shows more planar structure than 7-*tert*-butyl-1,3-bis(4-methoxyphenyl)pyrene,²² which is beneficial to extend the conjugated pathway and increase the absorption cross-section. Indeed, the molar absorption coefficient of **2c** ($\log \epsilon = 4.82$) is higher than 1,3-bis(4-methoxyphenyl)pyrene ($\log \epsilon = 4.51$). According to the reported,²⁷ due to the special electronic structure of pyrene, substituents at different position would cause a great difference of electron distribution. For example, the absorption of **2a–c** exhibited a great differences when compared to **3**. Clearly, substitution at the K-region (4,5,9,10-positions) exerts a greater influence on the $S_2 \leftarrow S_0$ excitation than substitution at the active sites of 1,3-position. The compounds **2a–c** with similar $S_2 \leftarrow S_0$ excitation coefficients ($\log \epsilon = 4.87$ for **2a**, 4.88 for **2b** and 4.82 for **2c**) are much larger than **3** ($\log \epsilon = 4.66$).²⁰

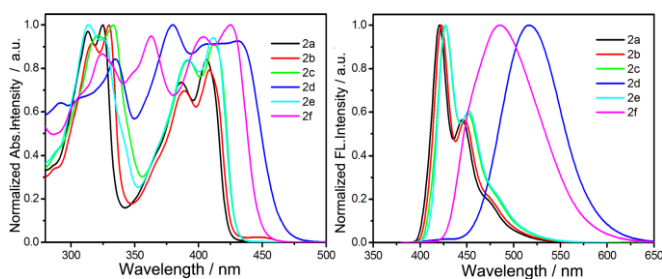


Figure 6. (a) Normalized UV-vis absorption and (b) fluorescence emission spectra of compounds **2** recorded in dichloromethane solutions at 10^{-5} – 10^{-6} M at 25 °C.

The fluorescence spectra of **2a–c** and **2e** exhibit a sharp peak at $\lambda_{em\ max} = 421, 423, 427$ and 427 nm with a shoulder. The emission spectra of **2d** and **2f** display a single broad peak at 517 nm and 485 nm, respectively, which indicates that the emission occurs from the lowest excited state with the largest oscillator strength. With the π -conjugation increasing, a gradual bathochromic shift in the $\lambda_{em\ max}$ is clearly observed in the order of **2a** \approx **2b** \approx **2c** \approx **2e** < **2f** < **2d**, implying that the energy gap between ground and excited states would decrease in this order. In this process, the ICT plays an important role in lowering the energy gap.²⁸ The optical properties are consisted with Kim's reports.²⁹ All of compounds show strong emission from deep blue to green color with high PL quantum yield (QYs) in the 0.80–0.94 range. The quantum yield of the titled compounds are higher than our previous reported by comparison of the series of 7-*tert*-butyl-1,3-diarylpyrenes.²² This was thought to be due to the increasing π -conjugation and delocalization of the electron density can improve the optical density, leading to strong FL emission in the solid-state.

Additionally, the fluorescence lifetime (τ_s) were measured in dichloromethane, and the results are listed in Table 2.

Furthermore, the effect on the optical properties of these compounds have been examined in solvents of various polarity,

such as cyclohexane, 1,4-dioxane, tetrahydrofuran (THF), dichloromethane (DCM) and *N,N*-dimethylformamide (DMF). The solvent dependence of the absorption and fluorescence spectra of **2** are displayed in Figure 7 and in the supporting information (Figure S3). The fluorescence spectra of **2d** and **2f** showed an obvious intermolecular charge transfer (ICT) emission band in different solvents with different polarity; for example, in **2d**, there was a remarkable solvatochromic color change from blue (432 nm in cyclohexane) to yellow (560 nm in DMF), owing to the presence of the terminal electron-donating *N,N*-dimethylamino groups ($-N(CH_3)_2$) which lead to a large change singlet excited-state dipole moment,³⁰ as the polarity of solvents increasing, the singlet excited states would decrease. The solvent effect of the absorption and fluorescence spectra was further evaluated by the Lippert-Mataga plot (Eqs. (1)–(2)),³¹ which is dependent on the Stokes shift ($\Delta\nu_{st}$) and the solvent parameter $\Delta f(\epsilon, n)$.³²

$$\Delta\nu = \frac{1}{4\pi\epsilon_0 h c a^3} \frac{2\Delta\mu^2}{h c R^3} \Delta f + \text{const} \quad (1)$$

Where $\Delta\nu = \nu_{abs} - \nu_{em}$ stands for Stokes shift, ν_{abs} is the wavenumber of maximum absorption, ν_{em} is the wavenumber of maximum emission, $\Delta\mu = \mu_e - \mu_g$ is the difference in the dipole moment of solute molecule between excited (μ_e) and ground (μ_g) states, h is the Planck's constant, R is the radius of the solvent cavity in which the fluorophore resides (Onsager cavity radius), and Δf is the orientation polarizability given by (Eq. 2).

$$\Delta f = \frac{\epsilon - 1}{2\epsilon + 1} - \frac{n^2 - 1}{2n^2 + 1} \quad (2)$$

Where ϵ is the static dielectric constant and n the refractive index of the solvent.

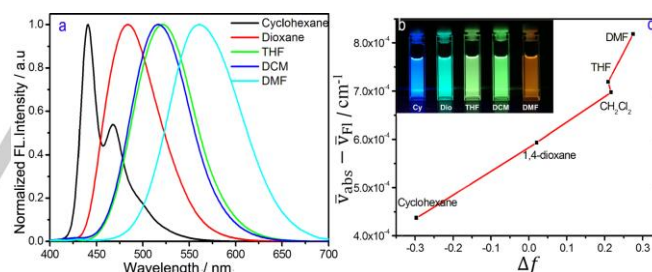


Figure 7. (a) Emission spectra of **2d** in cyclohexane, THF, CH_2Cl_2 , CH_3CN and DMF at 25 °C. (b) the solvatochromic colour change from blue to yellow, (c) Lippert-Mataga plots for compound **2d** ($-N(CH_3)_2$).

Similarly, the emission spectra of **2f** was red shifted show ca. 76 nm depending on the polarity of solvents (from 432 nm in cyclohexane to 497 nm in DMF) with obviously ICT characteristics. However, the emission maxima of **2a–c**, with the electronic-donating groups, and **2e** were slightly red shifted less 10 nm depending on the solvent polarity even in DMF (see supporting information). Although the compounds **2a–c** and **2e** possess weak CT characteristics, they display relatively high QYs compared with the others.

Electrochemical properties

The electrochemical properties of the title compounds **2a–e** were investigated by cyclic voltammetry (CV) in dichloromethane containing 0.1 M $n\text{Bu}_4\text{NPF}_6$ as the supporting electrolyte, with a scan rate of 100 mVs^{-1} at room temperature. As shown in Figure 8, all of the Y-shaped extended π -conjugated pyrene derivatives displayed an irreversible oxidation peak. In contrast, previous studies on similar Y-shaped pyrene molecules with aryl-substituted moieties have shown a quasi-reversible oxidation wave,²² which might be due to the terminal nature of the π -conjugated arylethynyl substitution effect on the electronic properties. For **2a–e**, the CV peaks for the positive potentials range from 1.23 to 1.28 V. According to the CVs and the UV-vis absorption, the highest occupied molecular orbital (HOMO) were estimated from the onset values of the first oxidation, and the optical energy gap (E_g) was derived from the UV-vis data. The HOMO energy levels for **2a–e** ranged from -5.28 to -5.34 eV, followed the empirical formula $\text{LUMO} = \text{HOMO} - E_g$, the LUMO levels of **2a–e** are located from -2.37 to -2.61 eV. Given the considerable HOMO and LUMO energy values of the compound, it might have potential use as a luminescent hole-transporting material in OLEDs.³³

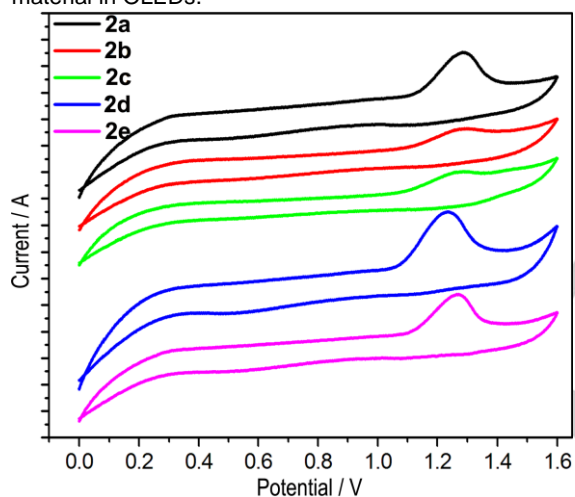


Figure 8. Cyclic voltammograms recorded for compounds **2a–e**.

Quantum chemistry calculations

To gain further insight into the electronic structures of the Y-shaped π -conjugated compounds **2**, DFT calculations were performed at the B3LYP/6-31G(d) level of theory using the Gaussian 2003 program.

The 3D-structures and energy density of the HOMO and LUMO levels of each material are displayed in Figure 9 and in the supporting information Figure S4. As the molecular geometries show, the substituent groups are almost coplanar with the pyrene core. Thus there is a close correlation between the quantum calculations and the single crystal X-ray diffraction results; minor differences of molecular geometry arise from the theoretical calculations being carried out in the “gas-phase”. On the other hand, the various substituent groups play a significant role for the HOMOs and LUMOs, for example, as the electron-releasing ability increases from **2a** to **2d**, the destabilization of

the HOMOs is greater than that of the LUMO, the HOMO levels are mostly located over the full molecular skeleton, whereas the LUMOs only spread in the center of pyrene rings; in contrast, with electron-withdrawing moieties, the LUMOs of **2e** and **2f** are almost fully localized on the entire molecular framework, and the HOMOs destabilized in the pyrene ring and a fragment of the phenyl groups. In addition, from the calculation data, we observed the energy gap of **2f** is close to **2d** with 2.83 eV, so both compounds exhibit similar UV spectra with a broad and strong absorption band in the 370–450 nm region. It is noteworthy that the HOMO-LUMO energy gaps of the title compounds **2** are lower than that previously reported for Y-shaped 1,3-bis(aryl)-functionalized pyrene species,²² due to the effect of arylethynyl moieties on the energies of the molecular orbitals.

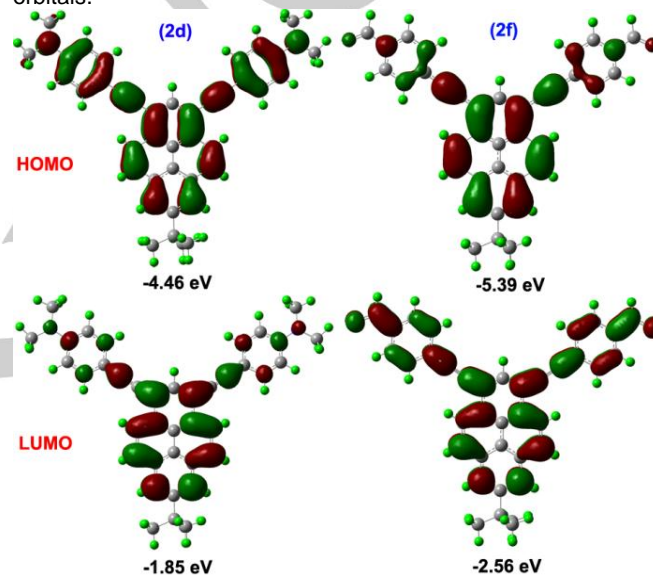


Figure 9. Selected computed molecular orbital plots (B3LYP/6-31G*) of the compounds **2d** and **2f**.

Conclusions

In summary, a series of Y-shaped arylethynyl-functionalized pyrenes **2** were synthesized by Pd-catalyzed Sonogashira coupling reaction in reasonable yield. The Y-shaped, extended π -conjugated pyrene derivatives display strong face-to-face π -stacking with off-set head-to-tail stacking as compared with a Y-shaped carbon-carbon single bond arylsubstituted pyrene.²² Furthermore, the effects of the substituents and their position on the crystal packing structure and photophysical properties of the chromophores has been evaluated. Compounds **2a–c** and **2e** in dichloromethane exhibited deep blue fluorescence with high quantum yield, while the chromophores **2d** and **2f** exhibit intermolecular charge-transfer (ICT) leading to intense optical absorbances over a wide spectral range. Strong fluorescence spectra of **2d** and **2f** show the maximum emission at 517 nm and 485 nm, respectively, with remarkable solvatochromic effects in polar solvents. Theoretical computation and experimental CV studies on their electrochemistry verify that Y-

shaped extended π -conjugated pyrenes **2** can be utilized in OLED devices as luminescent hole-transporting materials. In future, we will attempt to fabricate highly efficient OLED devices using these materials.

Acknowledgements ((optional))

This work was performed under the Cooperative Research Program of "Network Joint Research Center for Materials and Devices (Institute for Materials Chemistry and Engineering, Kyushu University)". We also would like to thank the EPSRC (overseas travel grant to C.R.), The Scientific Research Foundation for the Returned Overseas Chinese Scholars, State Education Ministry and The Scientific Research Common Program of Beijing Municipal Commission of Education for financial support (18190115/008).

Keywords: Pyrenes • Intramolecular charge-transfer • Single crystals • Luminescence material • Structure-property relationship

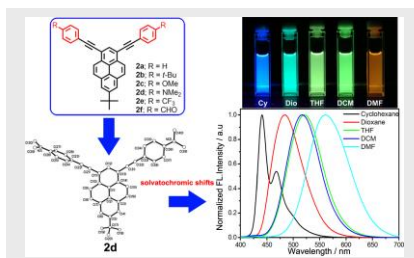
- [1] C.-L. Wang, H.-L. Dong, W.-P. Hu, Y.-Q. Liu, D.-B. Zhu, *Chem. Rev.* **2012**, *112*, 2208–2267.
- [2] H. Usta, A. Facchetti, T. Marks, *Acc. Chem. Res.* **2011**, *44*, 501–510.
- [3] A. Pietrangelo, B. O. Patrick, M. J. MacLachlan, M. O. Wolf, *J. Org. Chem.* **2009**, *74*, 4918–4926.
- [4] W. Wu, Y.-Q. Liu, D.-B. Zhu, *Chem. Soc. Rev.* **2010**, *39*, 1489–1502.
- [5] J. Li, Q. Zhang, *ACS Appl. Mater. Interfaces* **2015**, *7*, 28049–28062.
- [6] Y.-J. Cheng, S.-H. Yang, C.-S. Hsu, *Chem. Rev.* **2009**, *109*, 5868–5923.
- [7] a) A. R. Murphy, J. M. J. Fréchet, *Chem. Rev.* **2007**, *107*, 1066–1096; b) S. Mardanya, S. Karmakar, D. Mondal, S. Baitalik, *Dalton Trans.* **2015**, *44*, 15994–16012.
- [8] M. L. Tang, S. C. B. Mannsfeld, Y.-S. Sun, H. A. Becerril, Z. Bao, *J. Am. Chem. Soc.* **2009**, *131*, 882–883.
- [9] T. M. Figueira-Duarte, K. Müllen, *Chem. Rev.* **2011**, *111*, 7260–7314.
- [10] D. Karthik, K. R. J. Thomas, J.-H. Jou, S. Kumar, Y.-L. Chen, Y.-C. Jou, *RSC Adv.* **2015**, *5*, 8727–8738.
- [11] D. Cherccka, S.-J. Yoo, M. Baumgarten, J.-J. Kim, K. Müllen, *J. Mater. Chem. C* **2014**, *2*, 9083–9086.
- [12] J. K. Salunke, P. S., F. L. Wong, V. A. L. Roy, C. S. Lee, P. P. Wadgaonkar, *Phys. Chem. Chem. Phys.* **2014**, *16*, 23320–23328.
- [13] N. J. Jeon, J. Lee, J. H. Noh, M. K. Nazeeruddin, M. Grätzel, S. Il Seok, *J. Am. Chem. Soc.* **2013**, *135*, 19087–19090.
- [14] J.-Y. Hu, X. Feng, N. Seto, J.-H. Do, X. Zeng, Z. Tao, T. Yamato, *J. Mol. Struc.* **2013**, *1035*, 19–26.
- [15] X. Feng, J.-Y. Hu, F. Iwanaga, N. Seto, C. Redshaw, M. R. J. Elsegood, T. Yamao, *Org. Lett.* **2013**, *15*, 1318–1321.
- [16] S. Diring, F. Camerel, B. Donnio, T. Dintzer, S. Toffanin, R. Capelli, M. Muccini, R. Ziessel, *J. Am. Chem. Soc.* **2009**, *131*, 18177–18185.
- [17] Y. O. Lee, T. Pradhana, K. No, J. S. Kim, *Tetrahedron* **2012**, *68*, 1704–1711.
- [18] H. M. Kim, Y. O. Lee, C. S. Lim, J. S. Kim, B. R. Cho, *J. Org. Chem.* **2008**, *73*, 5127–5130.
- [19] T. Sato, M. Uejima, K. Tanaka, H. Kaji, C. Adachi, *J. Mater. Chem. C* **2015**, *3*, 870–878.
- [20] J.-Y. Hu, M. Era, M. R. J. Elsegood, T. Yamato, *Eur. J. Org. Chem.* **2010**, 72–79.
- [21] J.-Y. Hu, X.-L. Ni, X. Feng, M. Era, M. R. J. Elsegood, S. J. Teat, T. Yamato, *Org. Biomol. Chem.* **2012**, *10*, 2255–2262.
- [22] X. Feng, J.-Y. Hu, L. Yi, N. Seto, Z. Tao, C. Redshaw, M. R. J. Elsegood, T. Yamato, *Chem. Asian J.* **2012**, *7*, 2854–2863.
- [23] G. Cheng, B. Bonillo, R. S. Sprick, D. J. Adams, T. Hasell, A. I. Cooper, *Adv. Funct. Mater.* **2014**, *24*, 5219–5224.
- [24] M. Pope, C. E. Swenberg, *Electronic Processes in Organic Crystals and Polymers*; Oxford University Press: Oxford, **1999**, pp 48–53.
- [25] X. Feng, H. Du, K. Chen, X. Xiao, S.-X. Luo, S.-F. Xue, Y.-Q. Zhang, Q.-J. Zhu, Z. Tao, X.-Y. Zhang, G. Wei, *Cryst Growth Des.* **2010**, *10*, 2901–2907.
- [26] C.-G. Wang, S.-Y. Chen, K. Wang, S.-S. Zhao, J.-Y. Zhang, Y. Wang, *J. Phys. Chem. C* **2012**, *116*, 17796–17806.
- [27] A. G. Crawford, A. D. Dwyer, Z. Liu, A. Steffen, A. Beeby, L.-O. Pålsson, D. J. Tozer, T. B. Marder, *J. Am. Chem. Soc.* **2011**, *133*, 13349–13362.
- [28] a) S. Karmakar, D. Maity, S. Mardanya, S. Baitalik, *J. Phys. Chem. A* **2014**, *118*, 9397–9410; b) C. L. Droumaguet, A. Sourdon, E. Genin, O. Mongin, M. Blanchard-Desce, *Chem. Asian J.* **2013**, *8*, 2984–3001; c) R. Lartia; C. Allain. G. Bordeau, F. Schmidt, C. Fiorini-Debuisschert, F. Charra, M.-P. Teulade-Fichou, *J. Org. Chem.* **2008**, *73*, 1732–1744. d) X. Chen, X. Sang, Q. Zhang, *RSC Adv.* **2015**, *5*, 53211–53219.
- [29] a) H. M. Kim, Y. O. Lee, C. S. Lim, J. S. Kim, B. R. Cho, *J. Org. Chem.* **2008**, *73*, 5127–5130; b) Y. O. Lee, T. Pradhan, S. Yoo, T. H. Kim, J. Kim, J. S. Kim, *J. Org. Chem.* **2012**, *77*, 11007–11013; c) J. Sung, P. Kim, Y. O. Lee, J. S. Kim, D. J. Kim, *Phys. Chem. Lett.* **2011**, *2*, 818–823.
- [30] a) E. Sakuda, Y. Ando, A. Ito, N. Kitamura, *J. Phys. Chem. A* **2010**, *114*, 9144–9150; b) A. Ito, K. Kawanishi, E. Sakuda, N. Kitamura, *Chem. Eur. J.* **2014**, *20*, 3940–3953.
- [31] a) F. Han, L. Chi, W. Wu, X. Liang, M. Fu, J. Zhao, *J. Photochem. Photobio. A: Chem.* **2008**, *196*, 10–23; b) G.-J. Zhao, J.-Y. Liu, L.-C. Zhou, K.-L. Han, *J. Phys. Chem. B* **2007**, *111*, 8940–8945.
- [32] J. C. Sciano, *Handbook of Organic Photochemistry*; CRC Press: Boca Raton, FL, **1989**.
- [33] a) H. M. Duong, M. Bendikov, D. Steiger, Q. Zhang, G. Sonmez, J. Yamada, F. Wudl, *Org. Lett.* **2003**, *5*, 4433–4436; b) S. Mardanya, S. Karmakar, S. Das, S. Baitalik, *Sens. Actuators B Chem.* **2015**, *206*, 701–713.
- [34] G. A. Crosby, J. N. Demas, *J. Phys. Chem.* **1971**, *75*, 991–1024.
- [35] SAINT, SMART and APEX 2 (2000 & 2008) software for CCD diffractometers. Bruker AXS Inc., Madison, USA.
- [36] Programs CrysAlis-CCD and -RED, Oxford Diffraction Ltd., Abingdon, UK (2013).
- [37] L. Palatinus, G. Chapuis, *J. Appl. Cryst.* **2007**, *40*, 786–790.
- [38] G. M. Sheldrick, *Acta Crystallogr.* **2008**, *A64*, 112–122.

Entry for the Table of Contents (Please choose one layout)

Layout 1:

FULL PAPER

A series of high-efficiency luminescent material, namely 1,3-di(arylethynyl)-7-*tert*-butylpyrene, which were synthesized by a palladium-catalyzed Sonogashira coupling reaction. The detailed photophysical and electrochemical properties of titled compounds have been thoroughly investigated by experimental and theoretical.



Xing Feng,^{*[a,b]} Nobuyuki Seto,^[a]
Chuan-Zeng Wang,^[a] Taisuke
Matsumoto,^[c] Junji Tanaka,^[c] Xian-Fu
Wei,^[b] Mark R. J. Elsegood,^[d] Lynne
Horsburgh,^[d] Carl Redshaw,^[e] and
Takehiko Yamato^{*[a]}

Page No. – Page No.

Extended π -Conjugated Pyrene,
Derivatives: Structural,
Photophysical and Electrochemical
Properties

Layout 2:

FULL PAPER

((Insert TOC Graphic here; max. width: 11.5 cm; max. height: 2.5 cm))

Author(s), Corresponding Author(s)*

Page No. – Page No.

Title

Text for Table of Contents

1 Additional Author information for the electronic version of the article.
2

3 Xing Feng: 0000-0002-4273-979X
4 Author: ORCID identifier
5 Author: ORCID identifier
6
7
8
9
10
11
12
13
14
15
16
17
18
19
20
21
22
23
24
25
26
27
28
29
30
31
32
33
34
35
36
37
38
39
40
41
42
43
44
45
46
47
48
49
50
51
52
53
54
55
56
57
58
59
60
61
62
63
64
65

WILEY-VCH

Figure Captions:

Scheme 1. The synthetic route to π -conjugated pyrene derivatives **2**, and the cruciform-shaped and hand-shaped pyrenes **3** and **4** for comparison.

Figure 1. The molecular structures of **2cl**, **2d·CHCl₃** and **2f**.

Figure 2. X-ray crystal structure representations of **2cl**, illustrating (a) and (b) the co-facial π -stacking structures and (c) the principal intermolecular packing interactions.

Table 1. Summary of crystal data for the π -conjugated molecules **2cl**, **2cll**, **2d·CHCl₃** and **2f**.

Figure 3. X-ray crystal structure representations of **2d·CHCl₃**, illustrating (a) and (b) the co-facial π -stacking structures and (c) CHCl₃ molecules were captured in voids supported by C–H... π interactions.

Figure 4. X-ray crystal structure representations of **2f**, illustrating (a) and (b) the detail of the cofacial π -stacking structures and (c) the principal intermolecular packing interactions.

Table 2. The photophysical and electrochemical properties of compounds **2**.

Figure 5. The packing structure (a) side view and (b) top view for **3** and (c) side view and (d) top view for **4**.

Figure 6. (a) Normalized UV-vis absorption and (b) fluorescence emission spectra of compounds **2** recorded in dichloromethane solutions at $\sim 10^{-5}$ – 10^{-6} M at 25 °C.

Figure 7. (a) Emission spectra of **2d** in cyclohexane, THF, CH₂Cl₂, CH₃CN and DMF at 25 °C. (b) the solvatochromic colour change from blue to yellow, (c) Lippert-Mataga plots for compound **2d** (–N(CH₃)₂).

Figure 8. Cyclic voltammograms recorded for compounds **2a–e**.

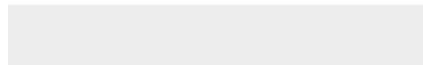
Figure 9. Selected computed molecular orbital plots (B3LYP/6-31G*) of the compounds **2d** and **2f**.

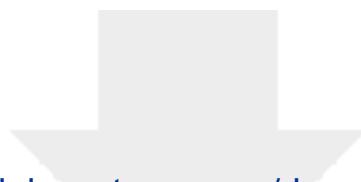


Click here to access/download

Supporting Information

3-slct201600605_SI-20160525.doc

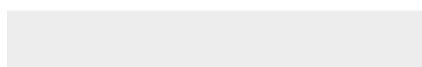
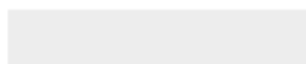


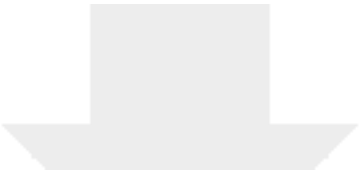


Click here to access/download

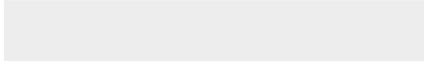
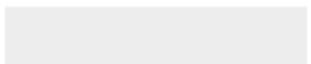
Additional Material - Author

4. 0524 Response to Reviewers Comments.docx



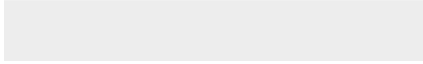


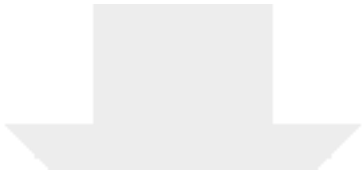
Click here to access/download
Supporting Information
2cl.cif



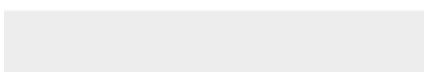
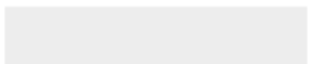


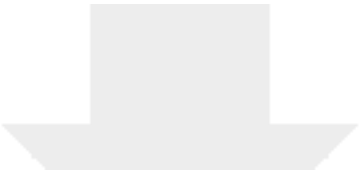
Click here to access/download
Supporting Information
2cll.cif





Click here to access/download
Supporting Information
2d.cif



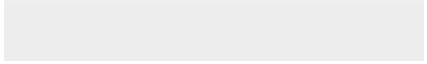
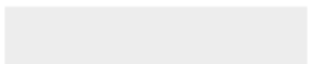


Click here to access/download
Supporting Information
2f.cif



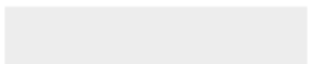


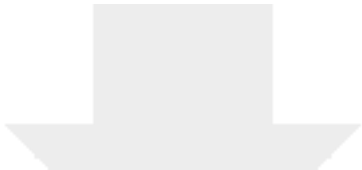
Click here to access/download
Supporting Information
2cl-checkcif.pdf



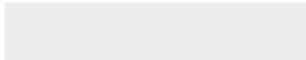


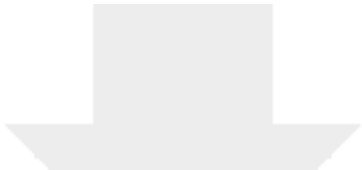
Click here to access/download
Supporting Information
2d-checkcif.pdf





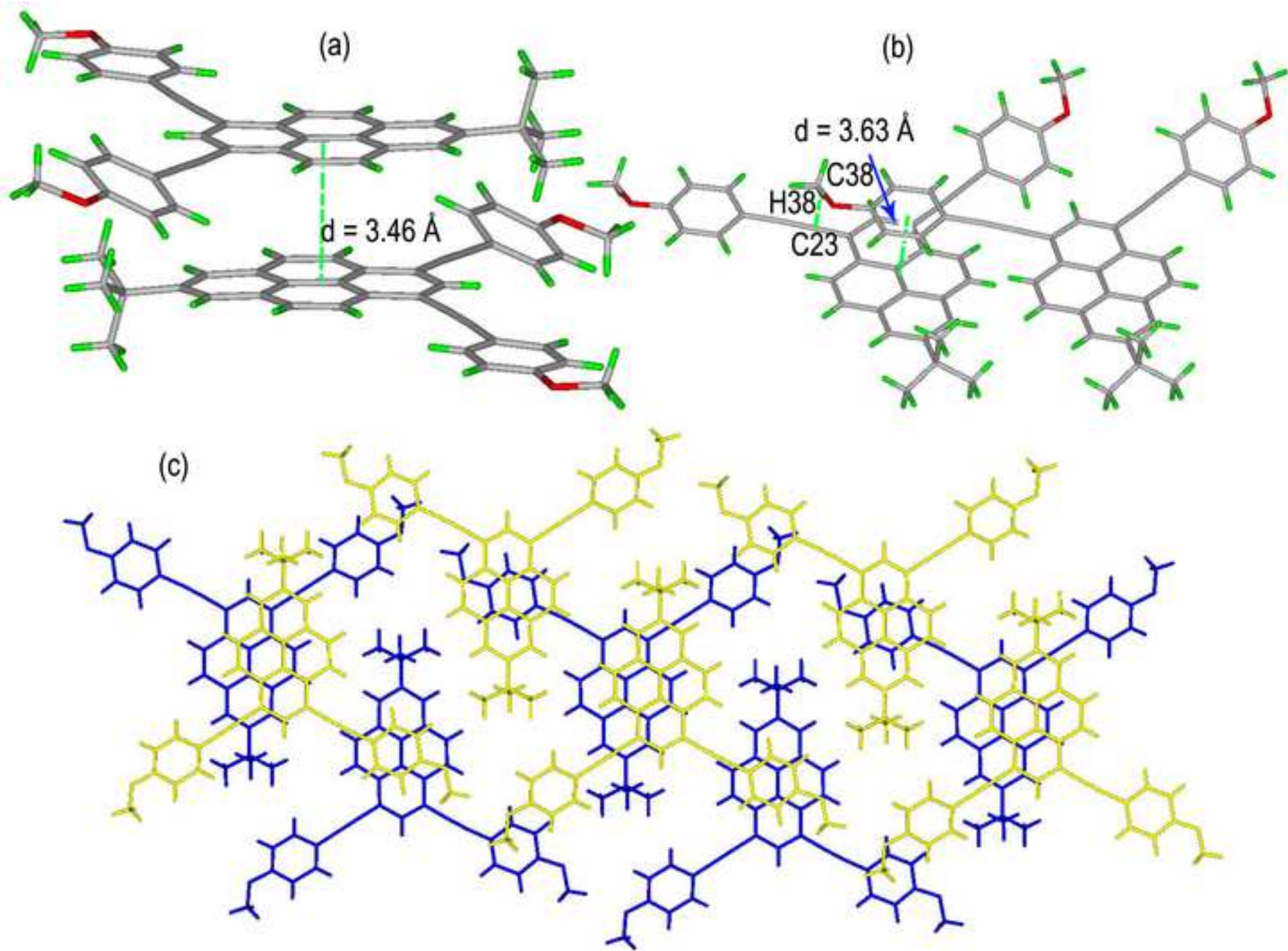
Click here to access/download
Supporting Information
2f-checkcif.pdf

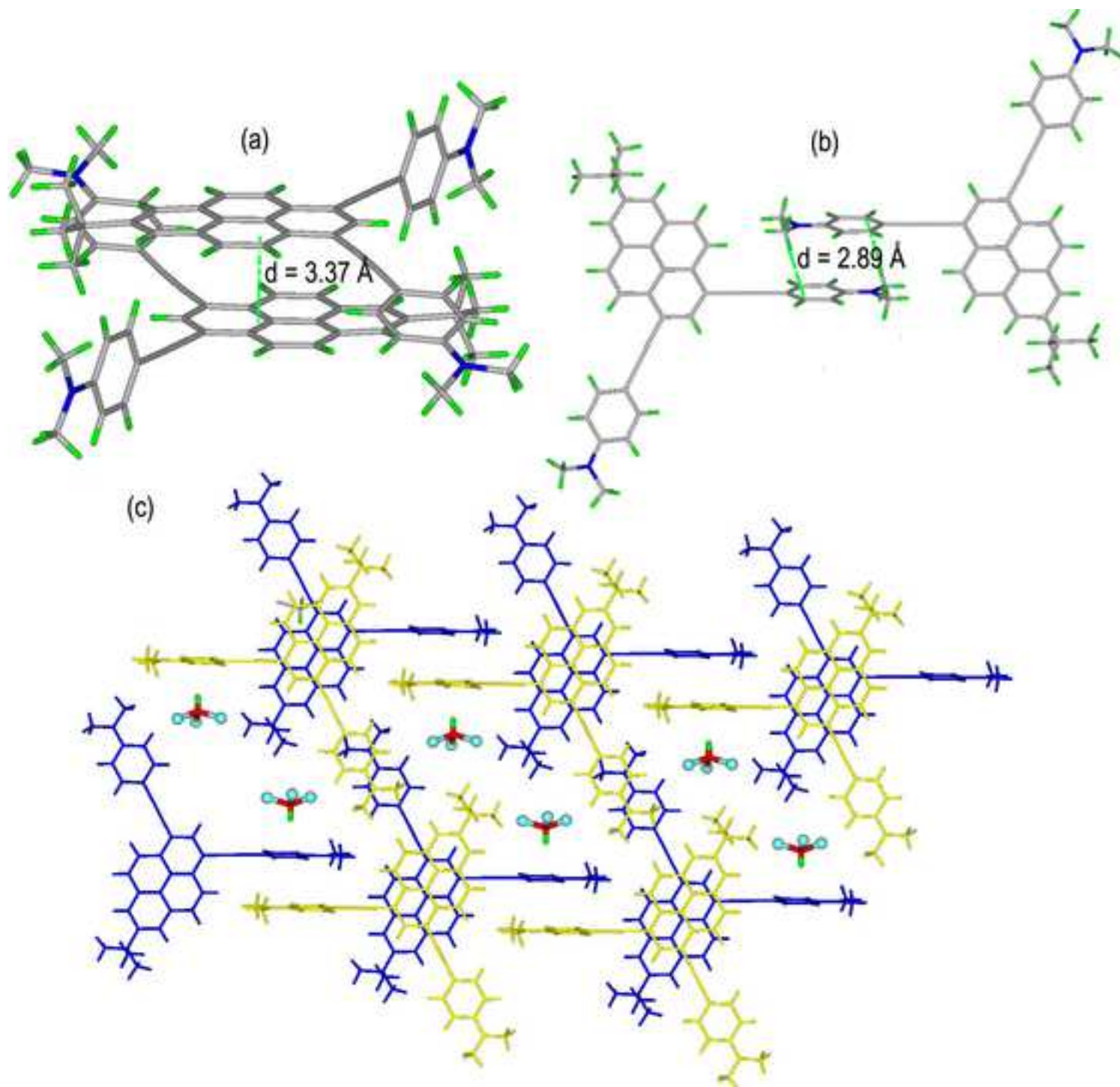


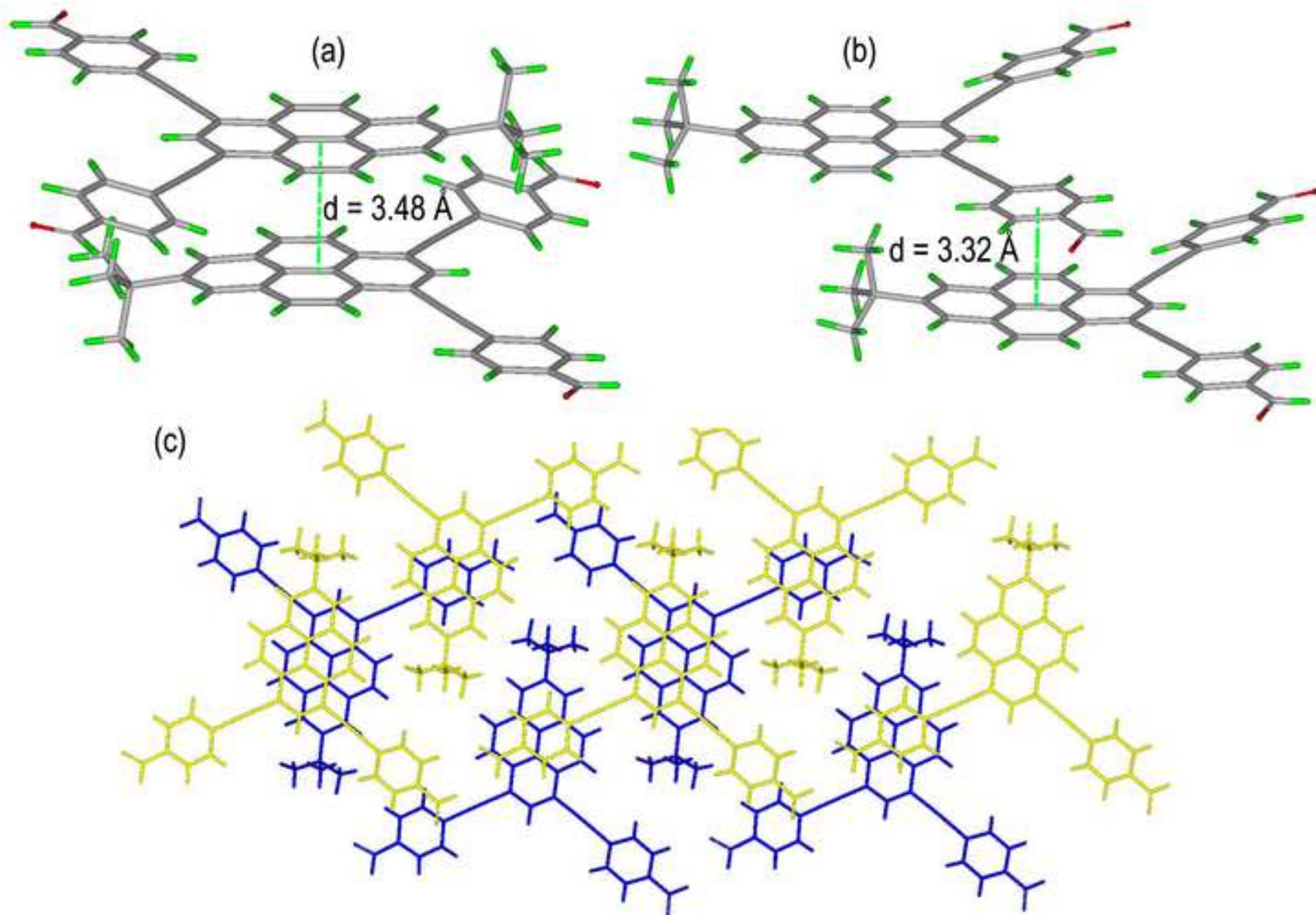


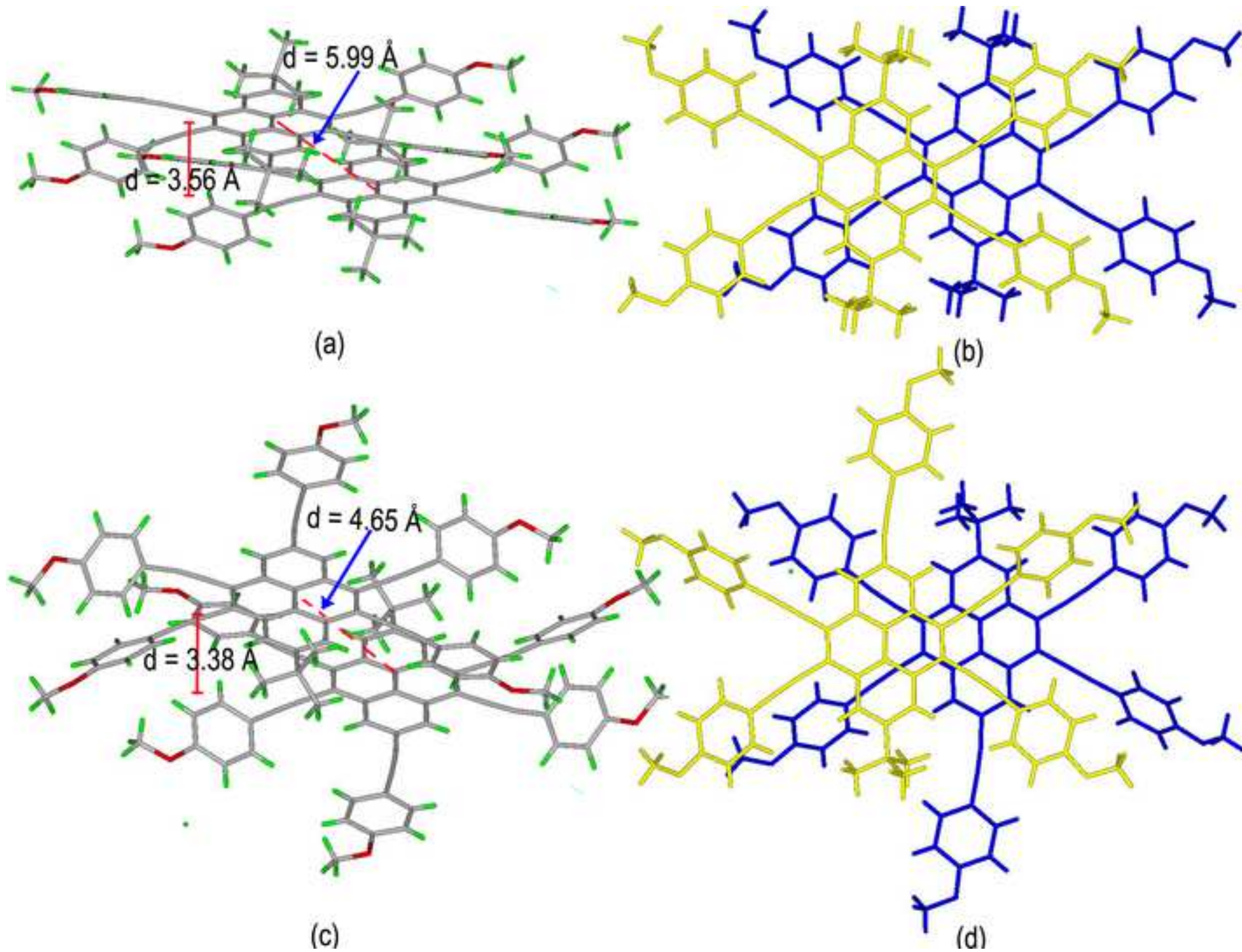
Click here to access/download
Supporting Information
2c11-checkcif.pdf

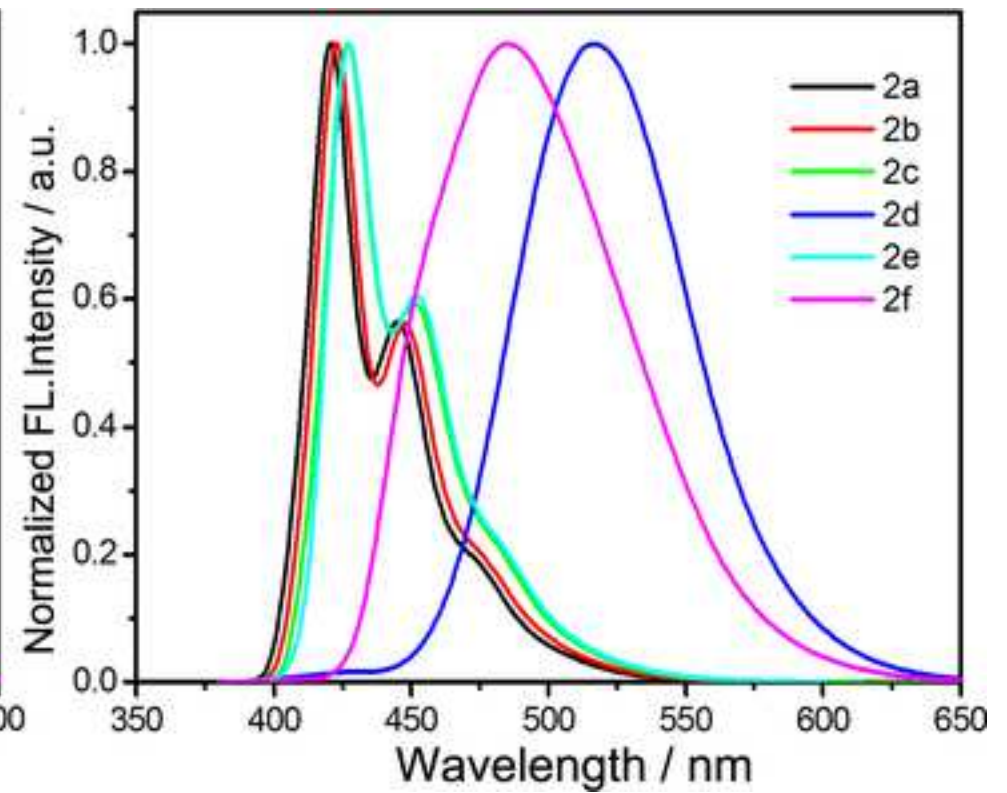
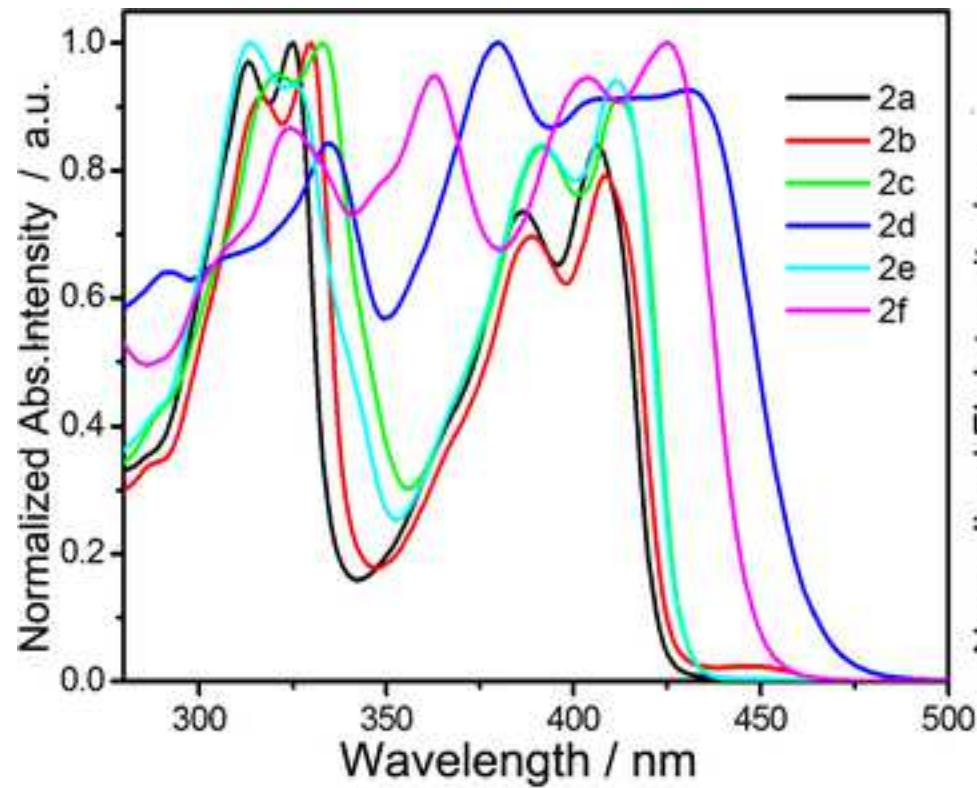


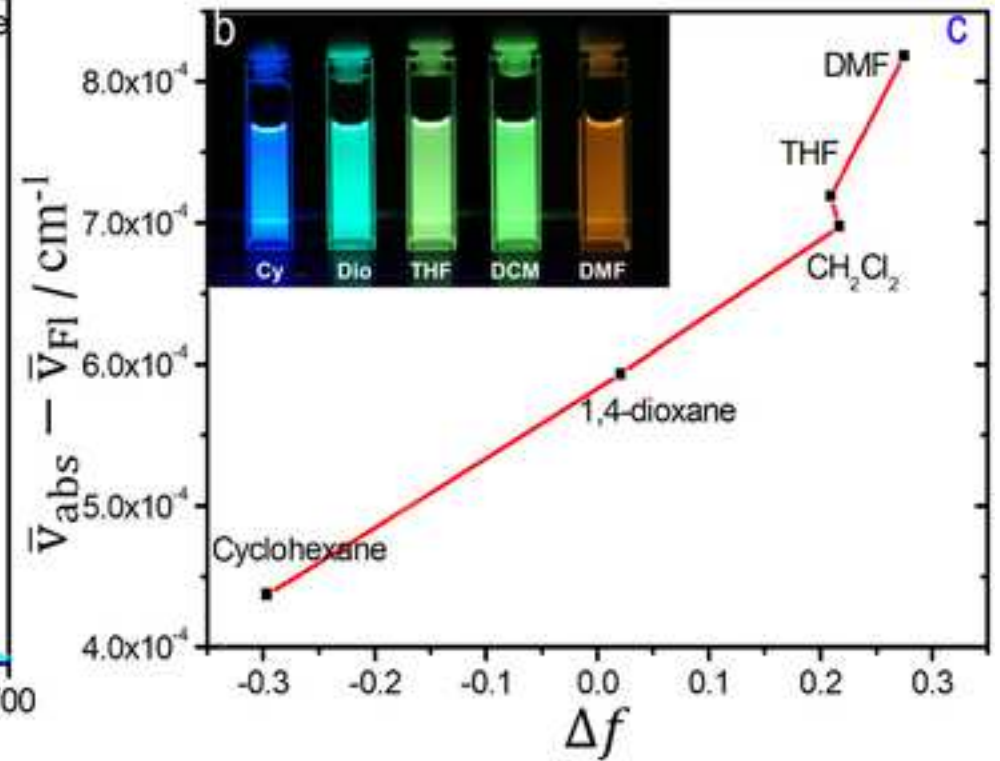
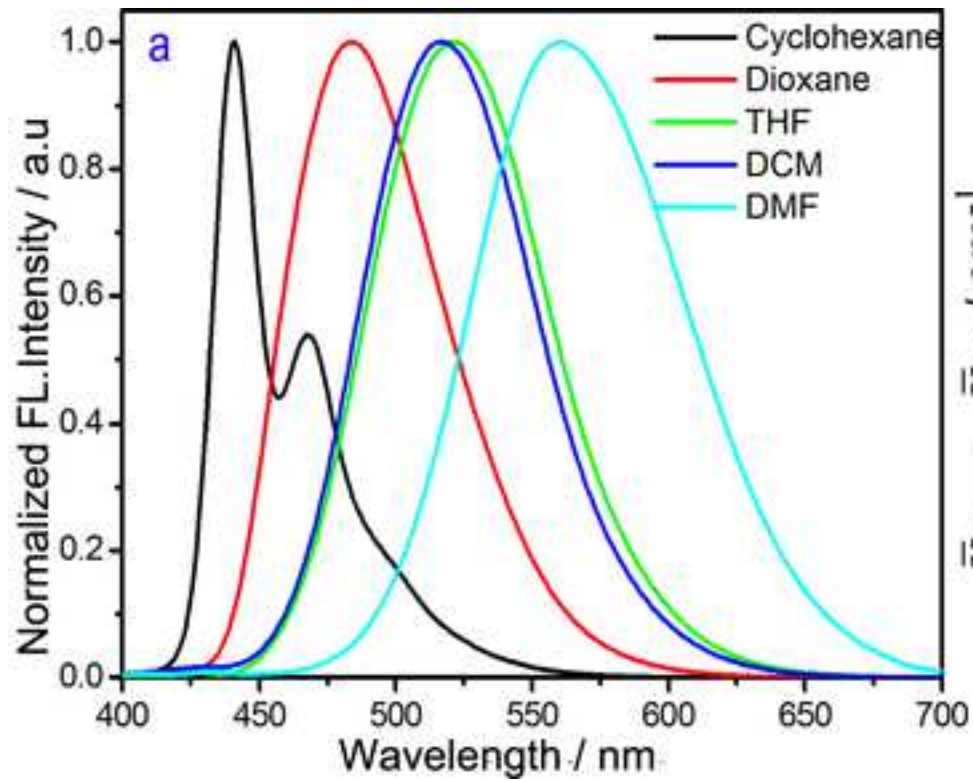


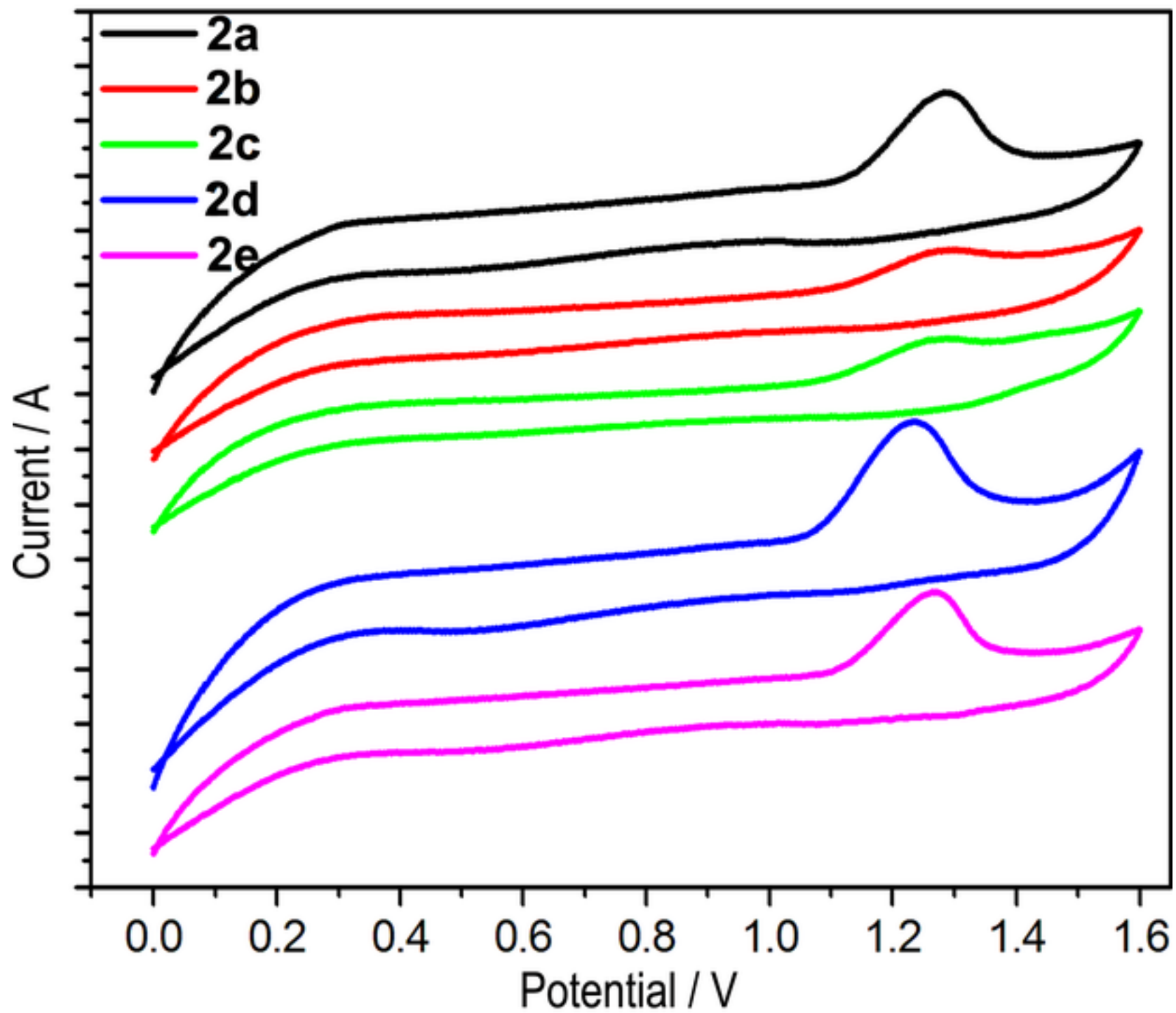


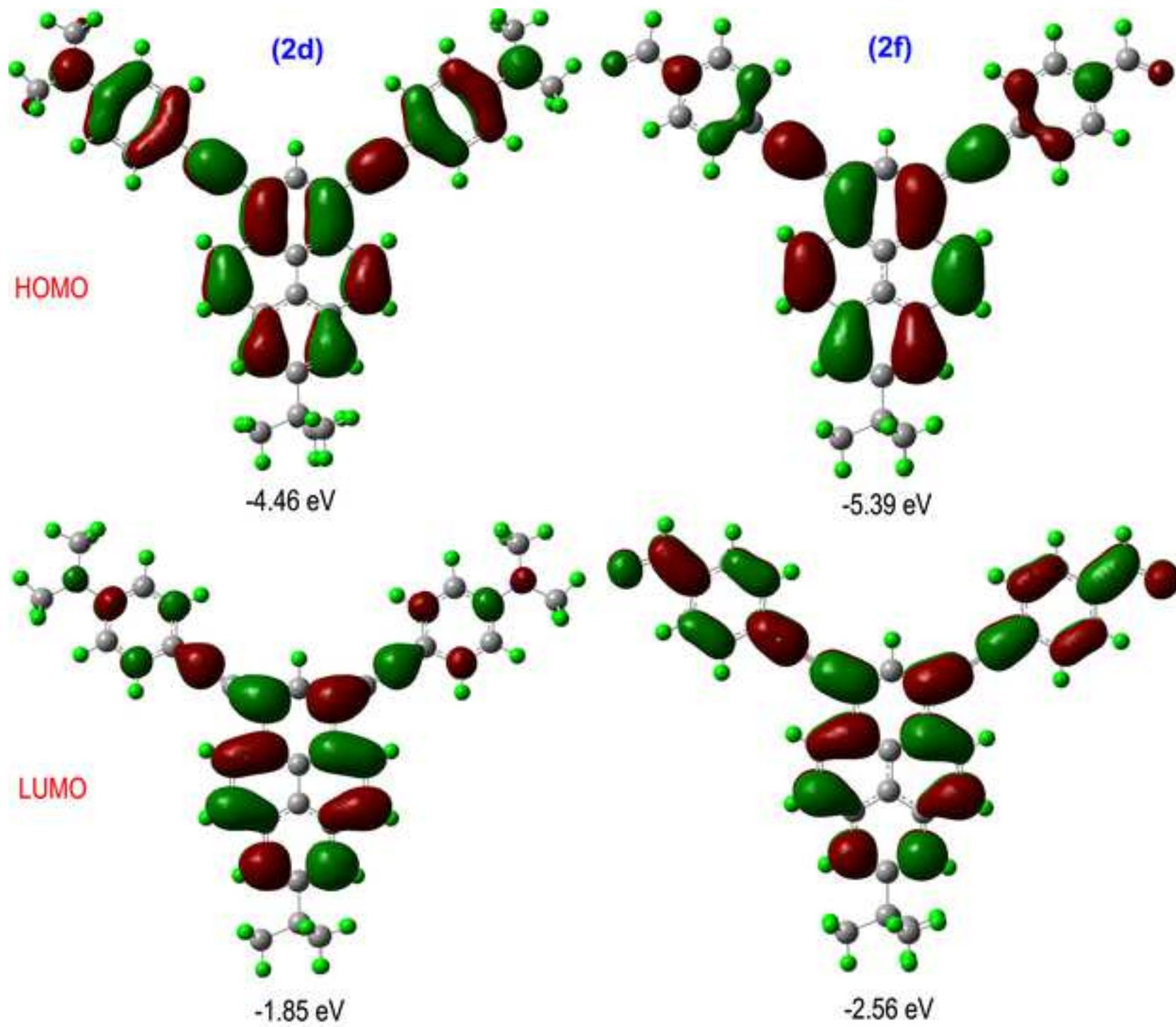


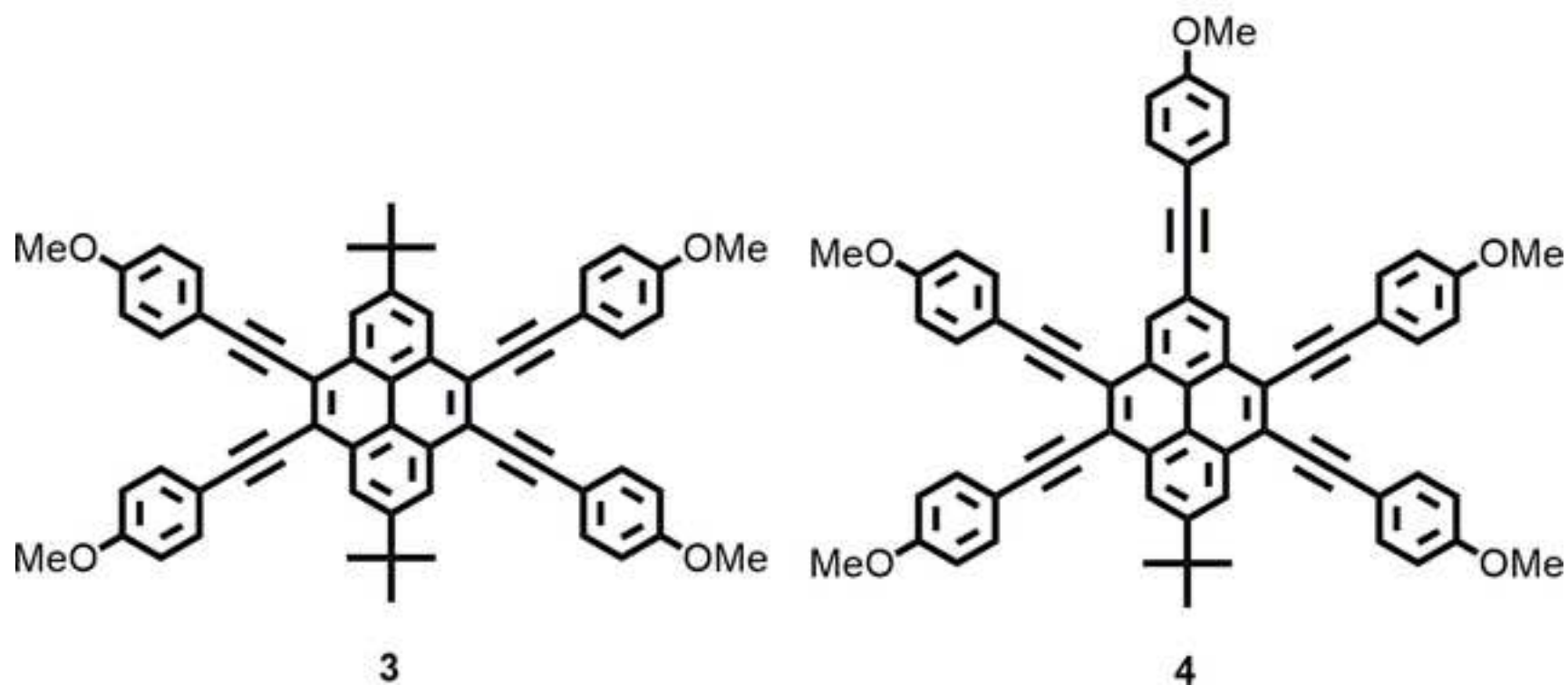
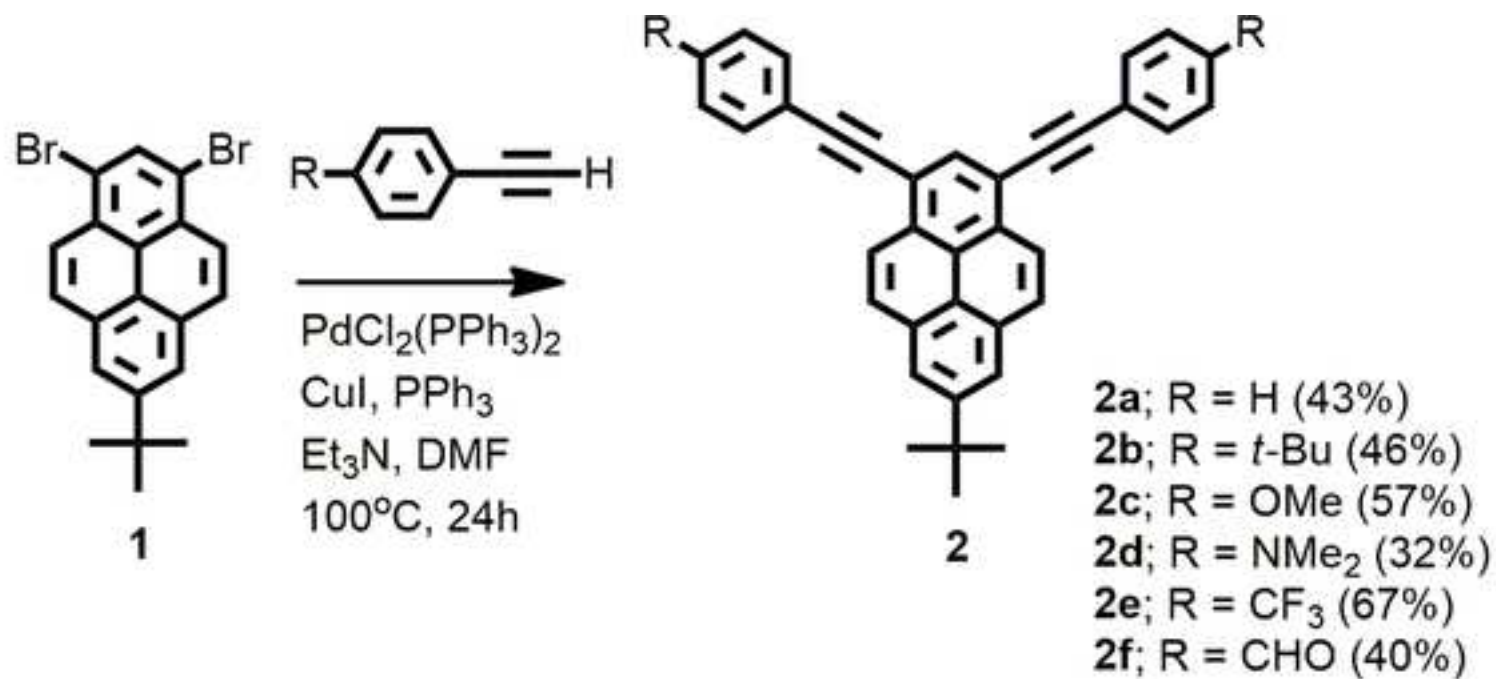


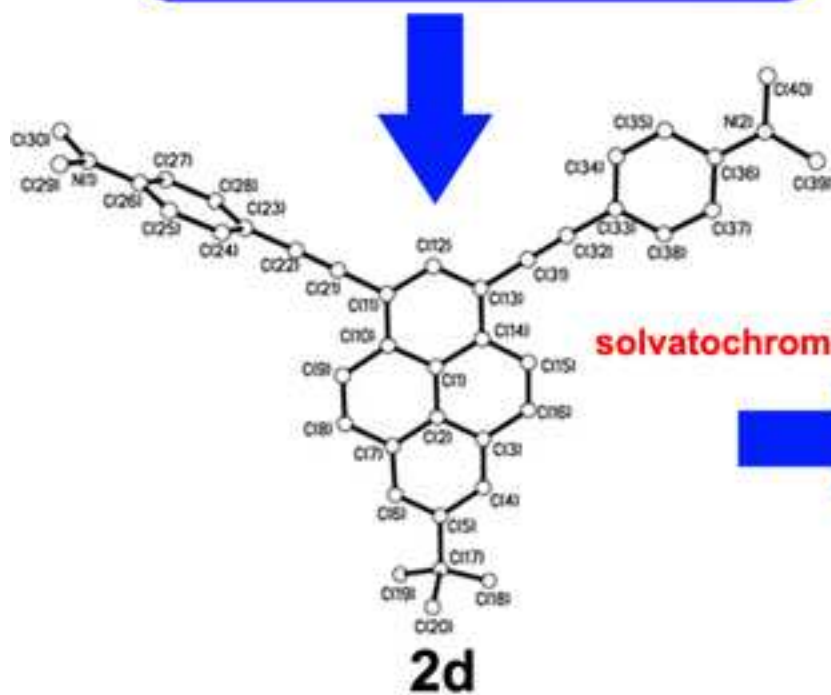
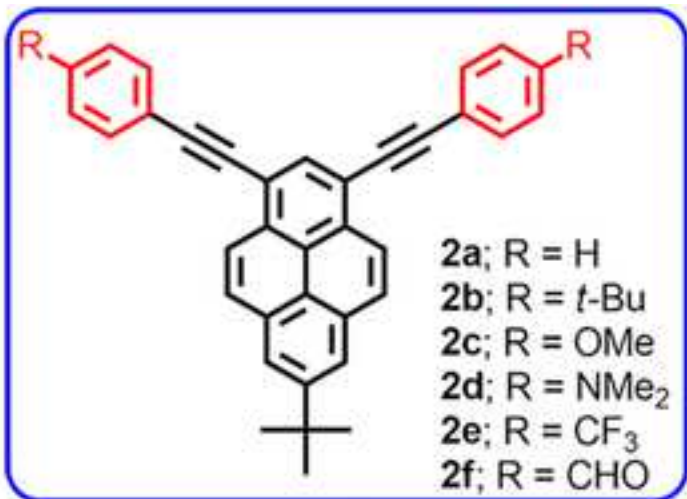












solvatochromic shifts

